Journal of Zhejiang University SCIENCE A
ISSN 1673-565X (Print); ISSN 1862-1775 (Online)
www.zju.edu.cn/jzus; www.springerlink.com
E-mail: jzus@zju.edu.cn

# Optimal design of Stewart platforms based on expanding the control bandwidth while considering the hydraulic system design*

Wei WANG, Hua-yong YANG, Jun ZOU†‡, Xiao-dong RUAN, Xin FU

(*State Key Laboratory of Fluid Power Transmission and Control, Zhejiang University, Hangzhou 310027, China*)

†E-mail: junzou@zju.edu.cn

Received Apr. 30, 2008; Revision accepted Oct. 30, 2008; Crosschecked Nov. 4, 2008

**Abstract:** We proposed an optimal design method to expand the bandwidth for the control of large hydraulic Stewart platform. The method is based on generalized natural frequency and takes hydraulic oil into consideration. A Lagrangian formulation which considers the whole leg inertia is presented to obtain the accurate equivalent mass matrix. Using the model, the effect of leg inertia and the influence of design parameters on the generalized natural frequency are investigated. Finally, numerical examples are presented to validate and confirm the efficiency of the mathematical model. The results show that the leg inertia, especially the piston part plays an important role in the dynamics. The optimum diameter ratio of the base to the moving platform is between 2 and 3, and the optimum joint angle ratio of the base to the moving platform is about 1. The smaller joint angles and a longer leg stroke are favorable for raising system frequencies. The system oil should be preprocessed for large platforms with a requirement for good dynamic performance.

**Key words:** Large Gough-Stewart platform, Optimal design, Control bandwidth, Leg inertia, Generalized natural frequency
**doi:**10.1631/jzus.A0820329 **Document code:** A **CLC number:** TP242

## INTRODUCTION

Compared with serial manipulators, parallel manipulators have a number of advantages such as higher rigidity and better positioning accuracy and load capacity. Therefore, parallel manipulators have been used in various applications. A six-degree-of-freedom (6-DOF) platform, first proposed by Gough in 1947 (Gough, 1956~1957), was later used by Stewart in his flight simulator. In the late 1970s, the Gough-Stewart platform was suggested for use as a parallel manipulator (Hunt, 1978).

In the design process of parallel manipulators, it is important and challenging to develop the optimum design (Merlet, 2002). Two issues are involved: performance evaluation and synthesis. Synthesis is important for determining the design parameters.

The performance of parallel manipulators depends heavily on their geometry and so much of the research on optimization has focused on criteria related to the workspace (Kumar, 1992). Other researchers chose to optimize the structural stiffness of the manipulator (Bhattacharya *et al.*, 1995), as that is one of the main advantages of a parallel compared with a serial configuration. Furthermore, some studies focused on optimization goals related to manipulability (Miller, 2004), dexterity (Pittens and Podhorodeski, 1993), payload (Gao *et al.*, 1997), conditioning index (Gosselin and Angeles, 1991) or accuracy (Ryu and Cha, 2001). These requirements are considered simultaneously in the optimum design (Arsenault and Boudreau, 2006). Different methods have been used to solve the optimum design problems including the cost-function approach, interval analysis (Hao and Merlet, 2005) and others (Zhang and Gosselin, 2002; Lou *et al.*, 2003; Smaili *et al.*, 2005). However, few optimization studies take the control

‡ Corresponding author

* Project supported by the National Basic Research Program (973) of China (No. 2006CB705400), the National Natural Science Foundation of China (No. 50705082) and the National Natural Science Fund for Distinguished Young Scholar (No. 50425518), China

problem into consideration. Shiller and Sundar (1991) used the motion time along the path as the cost function for optimization. Khatib and Bowling (1996) investigated the problem of manipulator design for increased dynamic performance, characterized by the inertia and acceleration properties of the end-effector. However, in applications with requirements for highly precise positioning and good dynamic performance (e.g., large flight simulators), the control of the platform is complicated and difficult. In general, the control of hydraulic actuators is more challenging than that of their electrical counterparts as they show significant nonlinear behavior. Factors such as nonlinear flow/pressure characteristics, variations in the trapped fluid volume due to piston motion, fluid compressibility, flow forces and their effects on the spool position and friction, all contribute to the significant nonlinear behavior. This will influence the actual control bandwidth, which in general is less than half of the natural frequency. To expand the theoretical bandwidth for the control, the natural frequency characteristics must be considered in the optimal design.

In this study, optimization based on generalized natural frequency has been carried out to expand the bandwidth for the control of a large hydraulic Stewart platform, taking into consideration the hydraulic system. The Lagrangian formulation, which considers the whole leg inertia, is developed to obtain the accurate equivalent mass matrix. An ADAMS model validates the efficiency of the mathematical model. The effect of leg inertia on dynamics is studied. Finally, the influence of design parameters and oil modulus on generalized natural frequency is investigated using the mathematical model.

## LAGRANGIAN FORMULATION

The dynamics of the Stewart platform is critically important. Several approaches have been proposed for dynamic analysis of Stewart platforms, including the Newton-Euler formulation, Lagrangian formulation and the Kane formulation. This optimization study aimed to expand the bandwidth for control using a method based on generalized natural frequency. The Lagrangian method is a direct way to obtain the equivalent mass matrix. Many previous studies (e.g., Lebret *et al.*, 1993; Wang, 2001) on dynamics analysis were based on simplified models, assuming that each leg of the Stewart platform can be represented by the center of leg mass where the mass is concentrated. Thus, the leg's kinetic energy comprises only the translational motion at its mass center, neglecting the rotary motion.

To ensure accuracy, the whole leg inertia is considered in this paper. The legs are decomposed into two parts: the fixed part (to the base) and the moving part (the piston part). The integral method is used to calculate the energy, including all the translational and rotational energy.

### Kinematics

The Stewart platform shown in Fig.1 is driven by hydraulic power.

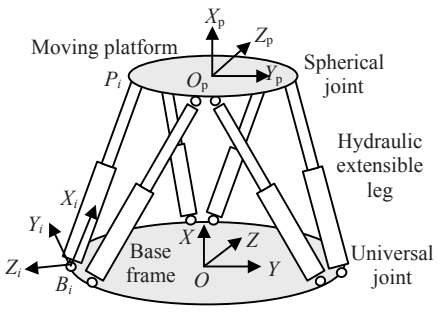


**Fig.1 Hydraulic Gough-Stewart platform**

Let $\boldsymbol{IJK}$ and $\boldsymbol{i}_i\boldsymbol{j}_i\boldsymbol{k}_i$ be the unit vectors of coordinates $O$-$XYZ$ and $B_i$-$X_iY_iZ_i$. The origin of leg coordinate system $B_i$-$X_iY_iZ_i$ is $B_i$. The $x$-axis points toward $P_i$. The $y$-axis is parallel to the cross product of vectors $\boldsymbol{i}_i$ and $-\boldsymbol{I}$. The $z$-axis of $B_i$-$X_iY_iZ_i$ is defined by the right-hand rule.

The transformation matrix $\boldsymbol{R}_i$ from the leg coordinate to the base coordinate can be obtained as in Pang and Shahinpoor (1994).

Let the rotation matrix be defined by the roll, pitch and yaw angles, namely, a rotation of $\varphi$ about the $x$-axis, followed by a rotation of $\psi$ about the $y$-axis, and a rotation of $\theta$ about the $z$-axis.

The length of the $i$th leg is given by

$$d_i = f_i(x_p, y_p, z_p, \psi, \theta, \phi). \tag{1}$$

This yields

$$\dot{\boldsymbol{d}}=\begin{bmatrix}\frac{\partial f_1}{\partial x_\mathrm{p}} & \frac{\partial f_1}{\partial y_\mathrm{p}} & \frac{\partial f_1}{\partial z_\mathrm{p}} & \frac{\partial f_1}{\partial \psi} & \frac{\partial f_1}{\partial \theta} & \frac{\partial f_1}{\partial \phi}\\ \frac{\partial f_2}{\partial x_\mathrm{p}} & \frac{\partial f_2}{\partial y_\mathrm{p}} & \frac{\partial f_2}{\partial z_\mathrm{p}} & \frac{\partial f_2}{\partial \psi} & \frac{\partial f_2}{\partial \theta} & \frac{\partial f_2}{\partial \phi}\\ \frac{\partial f_3}{\partial x_\mathrm{p}} & \frac{\partial f_3}{\partial y_\mathrm{p}} & \frac{\partial f_3}{\partial z_\mathrm{p}} & \frac{\partial f_3}{\partial \psi} & \frac{\partial f_3}{\partial \theta} & \frac{\partial f_3}{\partial \phi}\\ \frac{\partial f_4}{\partial x_\mathrm{p}} & \frac{\partial f_4}{\partial y_\mathrm{p}} & \frac{\partial f_4}{\partial z_\mathrm{p}} & \frac{\partial f_4}{\partial \psi} & \frac{\partial f_4}{\partial \theta} & \frac{\partial f_4}{\partial \phi}\\ \frac{\partial f_5}{\partial x_\mathrm{p}} & \frac{\partial f_5}{\partial y_\mathrm{p}} & \frac{\partial f_5}{\partial z_\mathrm{p}} & \frac{\partial f_5}{\partial \psi} & \frac{\partial f_5}{\partial \theta} & \frac{\partial f_5}{\partial \phi}\\ \frac{\partial f_6}{\partial x_\mathrm{p}} & \frac{\partial f_6}{\partial y_\mathrm{p}} & \frac{\partial f_6}{\partial z_\mathrm{p}} & \frac{\partial f_6}{\partial \psi} & \frac{\partial f_6}{\partial \theta} & \frac{\partial f_6}{\partial \phi}\end{bmatrix}\begin{bmatrix}\dot{x}_\mathrm{p}\\ \dot{y}_\mathrm{p}\\ \dot{z}_\mathrm{p}\\ \dot{\psi}\\ \dot{\theta}\\ \dot{\phi}\end{bmatrix}=\boldsymbol{D}\dot{\boldsymbol{q}}, \tag{2}$$

where $\boldsymbol{D}$ is the Jacobian matrix; $\dot{\boldsymbol{q}}=[\dot{x}_\mathrm{p}\ \dot{y}_\mathrm{p}\ \dot{z}_\mathrm{p}\ \dot{\psi}\ \dot{\theta}\ \dot{\phi}]^\mathrm{T}$.

**Piston part**

The velocity vector of the $i$th leg in coordinate system $\Sigma O$ can be written as

$$\begin{bmatrix}\dot{L}_{xi}\\ \dot{L}_{yi}\\ \dot{L}_{zi}\end{bmatrix}=\begin{bmatrix}\dot{x}_\mathrm{p}\\ \dot{y}_\mathrm{p}\\ \dot{z}_\mathrm{p}\end{bmatrix}+\dot{\boldsymbol{A}}_\mathrm{du}\begin{bmatrix}x_{\mathrm{u}i}\\ y_{\mathrm{u}i}\\ z_{\mathrm{u}i}\end{bmatrix}=\begin{bmatrix}\boldsymbol{J}_{xi}\\ \boldsymbol{J}_{yi}\\ \boldsymbol{J}_{zi}\end{bmatrix}\dot{\boldsymbol{q}}, \tag{3}$$

where $\dot{L}_{xi}=D(i,1),\dot{L}_{yi}=D(i,2),\dot{L}_{zi}=D(i,3)$; $\{x_\mathrm{p}\ y_\mathrm{p}\ z_\mathrm{p}\}$ is the moving platform center coordinate in $\Sigma O$; $\{x_{\mathrm{u}i}\ y_{\mathrm{u}i}\ z_{\mathrm{u}i}\}$ is the $i$th upper joint coordinate in $\Sigma O_\mathrm{p}$; and $\boldsymbol{A}_\mathrm{du}$ is the rotation matrix, $\boldsymbol{A}_\mathrm{du}=\boldsymbol{R}(y,\psi)\boldsymbol{R}(z,\theta)\boldsymbol{R}(x,\varphi)$.

In Fig.2, coordinates of particle $\mathrm{d}l_i$ in $\Sigma O$ can be obtained from

$$\begin{bmatrix}x_{\mathrm{l}i}\\ y_{\mathrm{l}i}\\ z_{\mathrm{l}i}\end{bmatrix}=\frac{(d_i-l_i)}{d_i}\left(\begin{bmatrix}x_i\\ y_i\\ z_i\end{bmatrix}-\begin{bmatrix}x_{\mathrm{d}i}\\ y_{\mathrm{d}i}\\ z_{\mathrm{d}i}\end{bmatrix}\right)+\begin{bmatrix}x_{\mathrm{d}i}\\ y_{\mathrm{d}i}\\ z_{\mathrm{d}i}\end{bmatrix}, \tag{4}$$

where $l_i$ is the length between $\mathrm{d}l_i$ and the $i$th upper joint, m; $\{x_{\mathrm{d}i}\ y_{\mathrm{d}i}\ z_{\mathrm{d}i}\}$ is the $i$th base joint coordinate in $\Sigma O$; $\{x_i\ y_i\ z_i\}$ is the $i$th upper joint coordinate in $\Sigma O$.

The total kinetic energy of the $i$th piston is

$$T_{\mathrm{l}i}=\int_0^{l_\mathrm{pis}}\frac{1}{2}\rho v_{\mathrm{l}i}^2\mathrm{d}l_i, \tag{5}$$

where $\rho=m_\mathrm{pis}/l_\mathrm{pis}$, $m_\mathrm{pis}$ is the piston mass, and $l_\mathrm{pis}$ is the piston length.

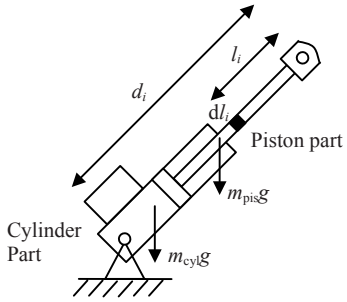


**Fig.2 Leg of the hydraulic Stewart platform**

**Cylinder part**

There is only rotation energy for the cylinder part. The angular velocity vector of the $i$th cylinder part is given by

$$\boldsymbol{\omega}_i=[\dot{\alpha}_i\ \dot{\beta}_i\ \dot{\gamma}_i]^\mathrm{T}. \tag{6}$$

The velocity of the $i$th upper joint can be written as

$$\boldsymbol{v}_i=\dot{\boldsymbol{d}}_i\cdot\boldsymbol{n}_{\mathrm{l}i}+\boldsymbol{\omega}_i\times\boldsymbol{d}_i, \tag{7}$$

where $\boldsymbol{n}_{\mathrm{l}i}$ is the unit vector along the $i$th leg.

No rotation is allowed about the leg axis, so taking the cross product of Eq.(7), the angular velocity of the cylinder part can be written as

$$\boldsymbol{\omega}_i=\boldsymbol{n}_{\mathrm{l}i}\times\boldsymbol{v}_i/d_i. \tag{8}$$

This yields

$$\boldsymbol{\omega}_i=\left(\frac{1}{d_i}\begin{bmatrix}d_{yi}\boldsymbol{J}_{zi}-d_{zi}\boldsymbol{J}_{yi}\\ d_{zi}\boldsymbol{J}_{xi}-d_{xi}\boldsymbol{J}_{zi}\\ d_{xi}\boldsymbol{J}_{yi}-d_{yi}\boldsymbol{J}_{xi}\end{bmatrix}\right)\dot{\boldsymbol{q}}=\boldsymbol{J}_\omega\dot{\boldsymbol{q}}. \tag{9}$$

Hence the total kinetic energy of the pistons is

$$\sum_{i=1}^{6}\frac{1}{2}\boldsymbol{\omega}_i^\mathrm{T}\boldsymbol{I}_i\boldsymbol{\omega}_i=\sum_{i=1}^{6}\frac{1}{2}\dot{\boldsymbol{q}}^\mathrm{T}\boldsymbol{J}_\omega^\mathrm{T}\boldsymbol{I}_i\boldsymbol{J}_\omega\dot{\boldsymbol{q}}, \tag{10}$$

where $\boldsymbol{I}_i=\boldsymbol{R}_i\boldsymbol{I}_i^{\mathrm{b}i}\boldsymbol{R}_i^\mathrm{T}$; $\boldsymbol{I}_i^{\mathrm{b}i}$ is the mass moment inertia of the $i$th cylinder about $B_i$ expressed in the leg coordinate system.

**Moving platform**

The moving platform's kinetic energy can be written as

$$K_{\mathrm{p}}=\frac{1}{2}\dot{\boldsymbol{q}}^{\mathrm{T}}\begin{bmatrix}\boldsymbol{M} & \boldsymbol{0}\\ \boldsymbol{0} & \boldsymbol{I}\end{bmatrix}\dot{\boldsymbol{q}}=\frac{1}{2}\dot{\boldsymbol{q}}^{\mathrm{T}}\boldsymbol{M}_{\mathrm{p}}\dot{\boldsymbol{q}}, \tag{11}$$

where $\boldsymbol{I}$ is inertia matrix of the moving platform in $\Sigma O$; $\boldsymbol{M}$ is the 3×3 mass diagonal matrix of the moving platform.

**Lagrangian formulation**

The potential energy of the moving platform can be written as

$$P_{\mathrm{p}}=m_{\mathrm{p}}gx_{\mathrm{p}}. \tag{12}$$

The leg potential energy is

$$P_{\mathrm{leg}}=g\sum_{i=1}^{6}\left(\left(m_{\mathrm{pis}}+(m_{\mathrm{cyl}}d_{\mathrm{cyl}}-m_{\mathrm{pis}}d_{\mathrm{pis}})/d_i\right)x_i\right), \tag{13}$$

where $m_{\mathrm{cyl}}$ is the cylinder mass, $d_{\mathrm{pis}}$ is the distance between the piston mass center and the corresponding upper joint, $d_{\mathrm{cyl}}$ is the distance between the cylinder mass center and the corresponding base joint, and $x_i$ is the $i$th upper joint's $x$ coordinate in the coordinate system $\Sigma O$.

Using the principle of virtual work and the Lagrange equation, the hydraulic driven force vector can be written as

$$\boldsymbol{F}=\boldsymbol{D}^{-\mathrm{T}}\left(\frac{\mathrm{d}}{\mathrm{d}t}\frac{\partial K}{\partial\dot{\boldsymbol{q}}}-\frac{\partial K}{\partial\boldsymbol{q}}+\frac{\partial P}{\partial\boldsymbol{q}}-\boldsymbol{F}_{\mathrm{ext}}\right), \tag{14}$$

where $K$ is the total kinetic energy, J; $P$ is the total potential energy, $P=P_{\mathrm{p}}+P_{\mathrm{leg}}$, J; $\boldsymbol{F}_{\mathrm{ext}}$ is the external generalized force vector.

## OPTIMUM METHOD BASED ON GENERALIZED NATURAL FREQUENCY

**Equivalent inertia matrix in $\Sigma O$**

From Eqs.(5), (10) and (11), the equivalent inertia matrix is

$$\boldsymbol{M}_{\mathrm{q}}=\boldsymbol{M}_{\mathrm{P}}+\sum_{i=1}^{6}\boldsymbol{I}_{\mathrm{li}}+\sum_{i=1}^{6}\boldsymbol{J}_{\omega}^{\mathrm{T}}\boldsymbol{I}_i\boldsymbol{J}_{\omega}, \tag{15}$$

where

$$\boldsymbol{I}_{\mathrm{li}}=\frac{1}{3}\rho\frac{l_{\mathrm{pis}}^3}{d_i^4}\boldsymbol{D}(i,:)^{\mathrm{T}}\boldsymbol{D}(i,:)\begin{bmatrix}x_i\\ y_i\\ z_i\end{bmatrix}^{\mathrm{T}}\begin{bmatrix}x_i\\ y_i\\ z_i\end{bmatrix}$$

$$-\frac{2\rho l_{\mathrm{pis}}^3}{3d_i^4}\boldsymbol{D}(i,:)^{\mathrm{T}}\boldsymbol{D}(i,:)\begin{bmatrix}x_i\\ y_i\\ z_i\end{bmatrix}^{\mathrm{T}}\begin{bmatrix}x_{\mathrm{d}i}\\ y_{\mathrm{d}i}\\ z_{\mathrm{d}i}\end{bmatrix}$$

$$+\frac{2\rho}{d_i^3}\left(\frac{1}{2}d_i l_{\mathrm{pis}}^2-\frac{1}{3}l_{\mathrm{pis}}^3\right)\boldsymbol{D}(i,:)^{\mathrm{T}}\left(\begin{bmatrix}x_i\\ y_i\\ z_i\end{bmatrix}^{\mathrm{T}}-\begin{bmatrix}x_{\mathrm{d}i}\\ y_{\mathrm{d}i}\\ z_{\mathrm{d}i}\end{bmatrix}^{\mathrm{T}}\right)\begin{bmatrix}\boldsymbol{J}_{xi}\\ \boldsymbol{J}_{yi}\\ \boldsymbol{J}_{zi}\end{bmatrix}$$

$$+\frac{\rho\boldsymbol{J}_i}{d_i^2}\left(d_i^2 l_{\mathrm{pis}}-d_i l_{\mathrm{pis}}{}^2+\frac{l_{\mathrm{pis}}^3}{3}\right)+\frac{1}{3}\frac{\rho l_{\mathrm{pis}}^3}{d_i^4}R^2\boldsymbol{D}(i,:)^{\mathrm{T}}\boldsymbol{D}(i,:),$$

where $\boldsymbol{J}_i=\boldsymbol{J}_{xi}{}^{\mathrm{T}}\boldsymbol{J}_{xi}+\boldsymbol{J}_{yi}{}^{\mathrm{T}}\boldsymbol{J}_{yi}+\boldsymbol{J}_{zi}{}^{\mathrm{T}}\boldsymbol{J}_{zi}$; $R$ is the radius of the base, m.

**Generalized natural frequency**

The Stewart platform is driven by hydraulic power. It is assumed that the mechanical part is rigid and that the hydraulic oil can be compressed like a spring. The stiffness of the hydraulic spring is defined as

$$k_{\mathrm{oil}}=\beta\left[\frac{A_1^2}{V_{\mathrm{oil1}}}+\frac{A_2^2}{V_{\mathrm{oil2}}}\right], \tag{16}$$

$$\boldsymbol{K}_{\mathrm{oil}}=k_{\mathrm{oil}}\boldsymbol{E}_6, \tag{17}$$

where $\beta$ is the oil bulk modulus, N/m$^2$; $A_1$ and $A_2$ are the effective driving area of the piston side and the rod side, m$^2$, respectively; $V_{\mathrm{oil1}}$ and $V_{\mathrm{oil2}}$ are the equivalent oil volume of the piston side and the rod side, m$^3$, respectively; and in $V_{\mathrm{oil1}}$ and $V_{\mathrm{oil2}}$ the oil volume in auxiliary pipes is considered; $\boldsymbol{E}_6$ is a 6×6 unit matrix.

According to the principle of virtual work, it follows that

$$\frac{1}{2}\delta\boldsymbol{q}^{\mathrm{T}}\boldsymbol{K}_{\mathrm{q}}\delta\boldsymbol{q}=\frac{1}{2}\delta\boldsymbol{l}^{\mathrm{T}}\boldsymbol{K}_{\mathrm{oil}}\delta\boldsymbol{l}=\frac{1}{2}\delta\boldsymbol{q}^{\mathrm{T}}\boldsymbol{D}^{\mathrm{T}}\boldsymbol{K}_{\mathrm{oil}}\boldsymbol{D}\,\delta\boldsymbol{q}. \tag{18}$$

This yields

$$\boldsymbol{K}_{\mathrm{q}} = \boldsymbol{D}^{\mathrm{T}} \boldsymbol{K}_{\mathrm{oil}} \boldsymbol{D}. \tag{19}$$

The generalized natural frequency vector on 6-DOF ($x\ y\ z\ \varphi\ \psi\ \theta$) is given by

$$\left\| \boldsymbol{K}_{\mathrm{q}} - (2\pi)^2 \boldsymbol{f}\boldsymbol{f}^{\mathrm{T}} \boldsymbol{M}_{\mathrm{q}} \right\| = 0, \tag{20}$$

$$\boldsymbol{f} = [f_1 \quad f_2 \quad f_3 \quad f_4 \quad f_5 \quad f_6]^{\mathrm{T}}. \tag{21}$$

**Optimization scheme**

For a large hydraulic Stewart platform, the key frequencies are the lowest natural frequency in the total workspace and the generalized natural frequency when all the actuators are at the mid-stroke. The aim of this design is to obtain the highest frequencies and to ensure that the natural frequencies are as close as possible when all the actuators are at their mid-stroke. The hydraulic oil should be considered in terms of the hydraulic system. This will be explained in detail, including figures, in the final section.

Many optimization studies are based on the cost function. It is important but difficult to determine the weights, which are basically determined empirically. This work is not based on the cost function. The steps in the optimization are as follows:

Step 1: Choose an initial set of design parameters. It can be roughly determined from the workspace requirement—the desired linear and angular accelerations at some velocity state.

Step 2: Determine the range of each design parameter and obtain the graphed results of their effects.

Step 3: Choose a new set of design parameters from Step 2 and obtain the task frequencies. If they are not satisfactory, change the design parameters and return to Step 2.

Step 4: Consider the hydraulic system design. The system oil can be preprocessed (Jin *et al.*, 2007) to improve the oil bulk modulus if necessary.

Step 5: Workspace verification and examination of other requirements.

In the paper, the configuration is representative for a group of nearby or symmetric configurations. Based on the method, design parameters will be determined that are more appropriate for the designer and that are related to the control and design of the hydraulic system.

## EFFECT OF LEG INERTIA

The design parameters of the Stewart platform are shown in Table 1.

**Table 1 Parameters of the Stewart platform**

| Parameter | Value |
|---|---|
| Upper diameter (m) | 2.1 |
| Base diameter (m) | 5.4 |
| Upper joints angle (°) | 21 |
| Base joints angle (°) | 21 |
| Initial height (m) | 2.5 |
| Length of the piston (m) | 2.3 |
| Length of the cylinder (m) | 2.2 |
| Mass of the moving platform (kg) | 300 |
| Mass of the piston (kg) | 200 |
| Mass of the cylinder (kg) | 350 |

The upper joints angle ($\alpha_{\mathrm{up}}$) and the base joints angle ($\alpha_{\mathrm{down}}$) are defined in Fig.3.

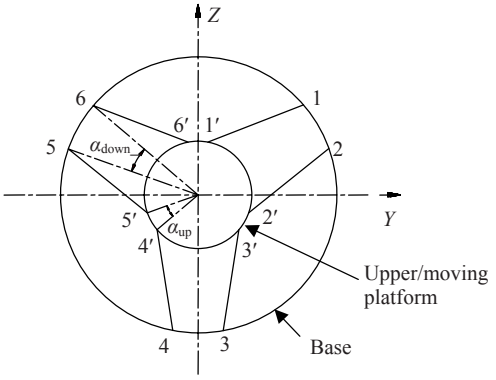


**Fig.3 Arrangement of the joints. Numbers 1~6 and 1′~6′ represent the base joints and upper joints, respectively**

Based on Table 1 and Eq.(15), the comparison between the current equivalent inertia matrix and the traditional matrix (in which it is assumed that each leg of the Stewart platform is represented by the center of leg mass where the mass is concentrated) is made when the platform is at the same position. The results are shown as the following two matrices (unit: kg):

$$\begin{bmatrix} 1073 & 0 & 0 & 0 & 0 & 0 \\ 0 & 938 & 0 & 0 & 44 & 0 \\ 0 & 0 & 938 & -44 & 0 & 0 \\ 0 & 0 & -44 & 592 & 0 & 0 \\ 0 & 44 & 0 & 0 & 592 & 0 \\ 0 & 0 & 0 & 0 & 0 & 1066 \end{bmatrix},$$

$$\begin{bmatrix} 529 & 0 & 0 & 0 & 0 & 0 \\ 0 & 627 & 0 & 0 & -32 & 0 \\ 0 & 0 & 627 & 32 & 0 & 0 \\ 0 & 0 & 32 & 291 & 0 & 0 \\ 0 & 32 & 0 & 0 & 291 & 0 \\ 0 & 0 & 0 & 0 & 0 & 669 \end{bmatrix}.$$

The former is the current inertia matrix and the latter is the traditional inertia matrix. Compared with the traditional inertia matrix, which considers only the translational part of the leg inertia, the current matrix considers the total leg inertia, including the rotary part.

The leg inertia will have definite effects on the dynamic driving forces. The current and the traditional models can be compared, as follows.

In Fig.4, the moving platform moves horizontally along the $z$-axis with a sinusoidal motion (100sin(πt) mm), while other velocities and accelerations remain zero. The curves, N-1, N-2 and N-3, are the results using the current inertia matrix model, and the curves, O-1, O-2 and O-3, are the results using the traditional model including only the translational part of the whole leg.

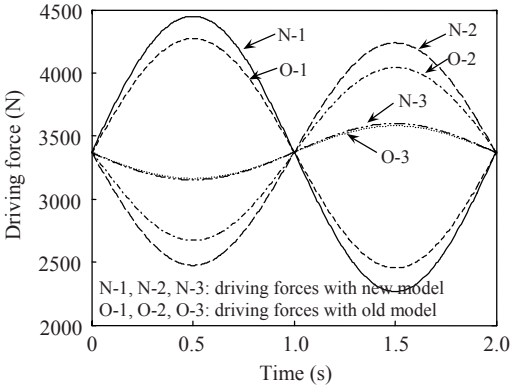


**Fig.4 Dynamic driving forces computed by models including whole leg energy and only the translational part of the leg**

From the above analysis, it can be observed that the piston part of the leg plays an important role in the dynamics and that the rotary inertia of the whole leg should not be neglected in the model.

## PARAMETERS OPTIMIZATION BASED ON THE NATURAL FREQUENCY

### Frequency verification

With the accurate inertia matrix, the generalized natural frequency of the Stewart platform can be obtained as in Eq.(20). With the mathematical model, the generalized natural frequency at the initial pose (2.5 m 0 m 0 m 0° 0° 0°) is [19.8487 42.1804 28.9790 41.1035 42.1804 19.8487] Hz.

An ADAMS model is built to validate the mathematical model, and the corresponding frequency is [19.8479 42.1809 28.9777 41.1033 42.1809 19.8479] Hz.

The generalized frequency in any pose of the workspace can be easily obtained with the mathematical model. It is difficult to do this using the ADAMS model, especially in searching for the lowest frequency in the total space. So the optimum work is obtained using the mathematical model.

### Influence of the design parameters on natural frequency

For a large Stewart platform with requirements of highly precise positioning and good dynamic performance, the lowest natural frequency in the total workspace and the generalized natural frequencies when all the actuators are at the mid-stroke, are the key frequencies. The dynamic performance of the platform is the greatest when all actuators are at the mid-stroke, and the Stewart platform often works around that position.

The influence of the ratio ($r_1$) of leg mass to moving platform and the ratio ($r_2$) of cylinder mass to piston is shown in Figs.5 and 6 (In Figs.5~8, 10, 11, 13, and 15, curves 1~4 represent the six frequencies when all the actuators are at the mid-stroke and curve 5 represents the lowest frequency in the workspace). In Figs.5 and 6, the key frequencies decrease with the increase of the mass ratios. However, they are nonlinear with ratio $r_1$ and the frequencies decrease linearly and only slightly with ratio $r_2$. It can be concluded that the influence of mass ratio $r_2$ is less important than that of $r_1$, and that the leg inertia can be designed mainly on the cylinder part.

The influence of the diameter ratio of the base to the moving platform is shown in Figs.7 and 8. Three evaluation indexes of the six mid-stroke generalized frequencies are introduced: mean arithmetical value, unbiased variance and the ratio of maximum to minimum frequency. The aim is to obtain a higher mean arithmetical value, lower unbiased variance and lower ratio of maximum to minimum

frequency.

Figs.7 and 8 indicate that the influence of the diameters is highly non-linear. The lowest frequency in the workspace (curve 5) reaches a peak (12 Hz) when the diameter ratio is about 2.2, and the highest point (18 Hz) of curve 4 appears when the ratio is about 2.8. All the task frequencies decrease rapidly when the diameter ratio is about 3.0, especially for the four lower frequencies.

Fig.9 shows the influence of diameter ratio on evaluation indexes. The optimum diameter ratio is in the range of 2.0~3.0 or 4.0~5.0. Considering the lowest frequency in the workspace (Fig.8), a diameter ratio between 2.0 and 3.0 is the best.

The influence of the angle ratio of base joints to upper joints is shown in Figs.10~12.

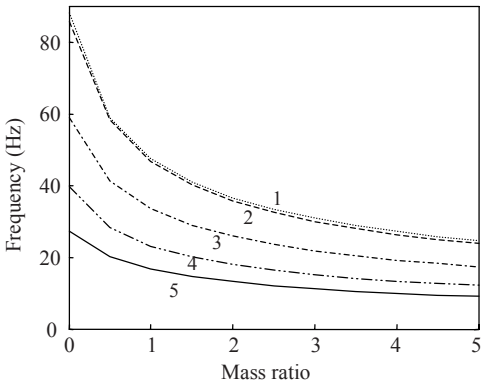


**Fig.5 Influence of the ratio ($r_1$) of the total leg mass to that of the moving platform on frequency**

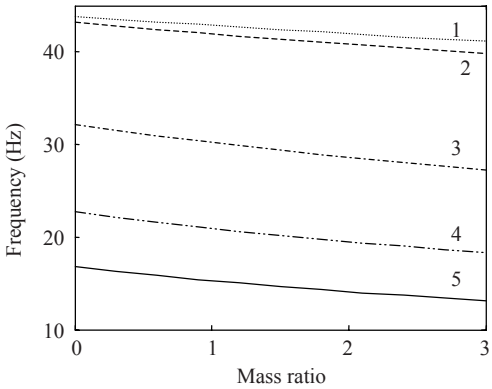


**Fig.6 Influence of the ratio ($r_2$) of cylinder mass to piston mass on frequency**

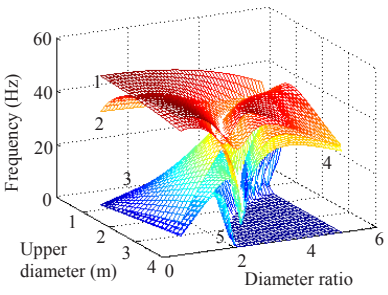


**Fig.7 Influence of the moving platform diameter and the diameter ratio of base to moving platform on frequency**

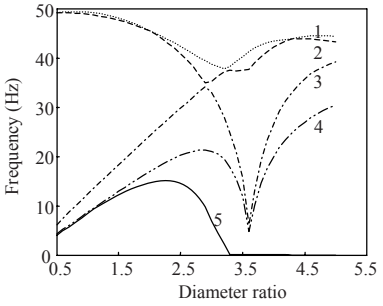


**Fig.8 Influence of the diameter ratio of base to moving platform on frequency**

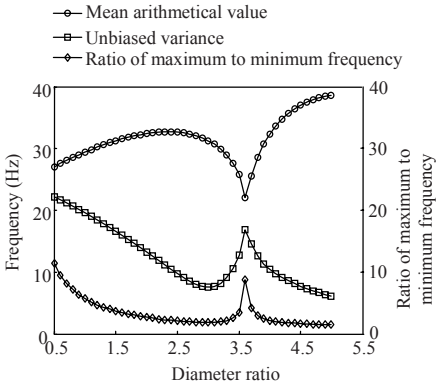


**Fig.9 Influence of the diameter ratio of base to moving platform on evaluation indexes**

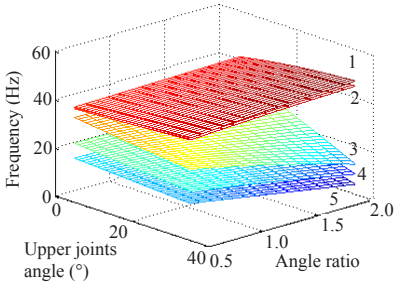


**Fig.10 Influence of the upper joints angle and the angle ratio of base joints to upper joints on frequency**

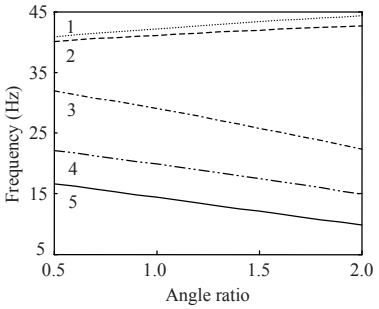


**Fig.11 Influence of the angle ratio of base joints to upper joints on frequency**

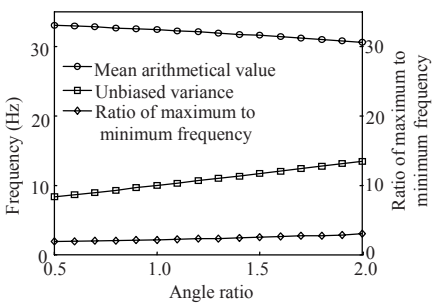


**Fig.12 Influence of the angle ratio of base joints to upper joints on evaluation indexes**

From Figs.10~12, the influence of the angles on natural frequencies and evaluation indexes are linear. An increase in the upper joints angle and the angle ratio makes the three highest frequencies (curves 1 and 2) increase slightly, but lowers the other three frequencies more (curves 3, 4 and 5).

Fig.12 shows clearly that a smaller angle ratio gives a higher mean arithmetical value and lower unbiased variance, while the ratio of maximum to minimum frequency remains steady. So the smaller joint angles and angle ratios are favorable for raising the task frequencies. For all the task frequencies considered, the ratio of base joints angle to that of the upper joints is best around 1.0.

The influence of the leg stroke is shown in Figs.13 and 14.

It can be seen that the leg stroke influences the lowest frequency more than the mid-stroke frequencies. The longer leg stroke is favorable for raising the lowest frequency in the total workspace with a minimal sacrifice of other requirements.

From Eq.(16), the influence of the oil modulus is the same as that of the effective driving area (the oil volume is proportional to each driving area). Both are of great benefit for raising all frequencies simultaneously. However, the increase in effective driving area may add to the difficulty of hydraulic design (leakage, friction and system flow rate supply), and the system mass will increase.

Figs.15 and 16 show the effect of the oil bulk modulus. The higher oil bulk modulus is favorable for raising all the target frequencies. The effective oil bulk modulus in practice is about $7.0\times10^9$ N/m$^2$ for the gas dissolving in the oil. With some vacuum-pumping de-aerating devices (Jin *et al.*, 2007), the hydraulic oil bulk modulus can be raised by more than $1.0\times10^{10}$ N/m$^2$. So, if necessary, the oil can be pre-processed. This is a more appropriate method than increasing the driving area.

## CONCLUSION

We presented an optimal design method, based on generalized natural frequency, aiming to expand the bandwidth for the control of large hydraulic

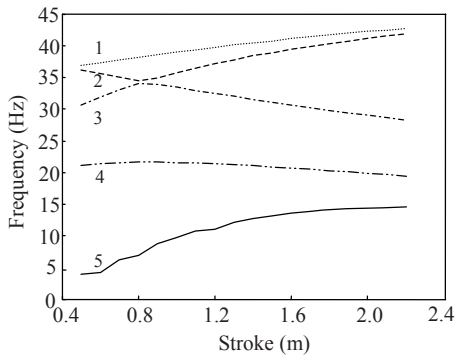


**Fig.13 Influence of leg stroke on frequency**

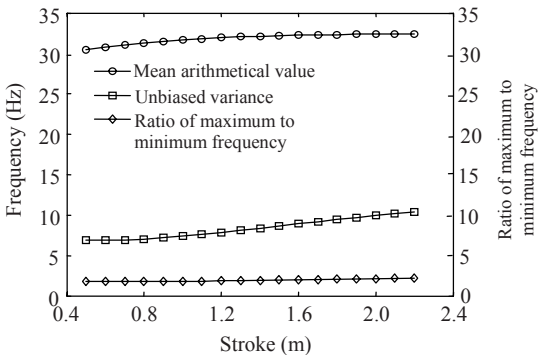


**Fig.14 Influence of leg stroke on evaluation indexes**

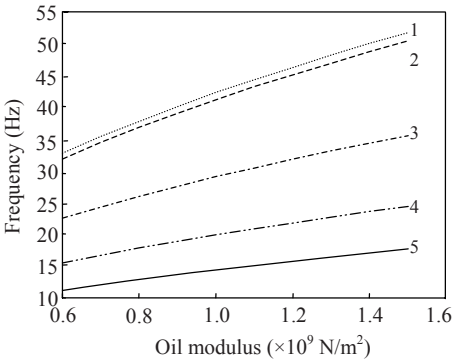


**Fig.15 Influence of oil modulus on frequency**

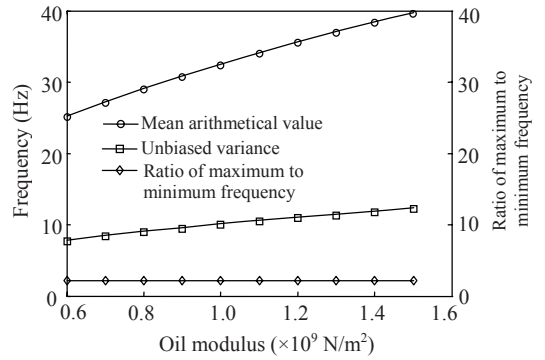


**Fig.16 Influence of oil modulus on evaluation indexes**

Stewart platforms. The hydraulic system is also considered. The ADAMS model validates and confirms the efficiency of the current model. Numerical examples were given which led to the following conclusions:

(1) The piston part of the leg plays a more important role than the cylinder part, and the rotary inertia of the whole leg should be considered with large platforms. Moreover, the influence of the ratio of leg mass to upper platform mass is more important than that of cylinder mass to piston mass.

(2) The optimum diameter ratio of the base to the moving platform is between 2.0 and 3.0.

(3) Smaller joint angles and angle ratio of the base joints to upper joints are favorable for raising the task frequencies. The joint angle ratio is best around 1.

(4) A longer leg stroke is favorable for raising the lowest frequency in the total workspace.

(5) The influence of the oil modulus is the same as that of the effective driving area, and provides a more effective method than increasing the driving area.

This optimization method can be used with other requirements. It is an efficient method for obtaining a compact hydraulic Stewart platform with higher bandwidth, and is suitable for the optimum design of other hydraulic parallel manipulators.

## References


Arsenault, M., Boudreau, R., 2006. Synthesis of planar parallel mechanisms while considering workspace, dexterity, stiffness and singularity avoidance. *Journal of Mechanical Design*, **128**(1):69-78. [doi:10.1115/1.2121747]

Bhattacharya, S., Hatwal, H., Ghosh, A., 1995. On the optimum design of Stewart platform type parallel manipulators. *Robotica*, **13**(2):133-140.

Gao, F., Guy, F., Gruver, W.A., 1997. Criteria Based Analysis and Design of Three-degree-of-freedom Planar Robotic Manipulators. Proceedings of IEEE International Conference on Robotics and Automation, New Mexico, **1**(468-473). [doi:10.1109/ROBOT.1997.620081]

Gosselin, C., Angeles, J., 1991. A global performance index for the kinematic optimization of robotic manipulators. *Journal of Mechanical Design*, **113**(3):220-226. [doi:10.1115/1.2912772]

Gough, V.E., 1956~1957. Contribution to discussion of papers on research in automobile stability, control and tyre performance. *Proceedings of the Institution of Mechanical Engineers: Auto Division*, **171**:392-395.

Hao, F., Merlet, J.P., 2005. Multi-criteria optimal design of parallel manipulators based on interval analysis. *Mechanism and Machine Theory*, **40**(2):157-171. [doi:10.1016/j.mechmachtheory.2004.07.002]

Hunt, K.H., 1978. Kinematic Geometry of Mechanisms. Oxford University Press, Oxford.

Jin, Y.L, Gong, G.F., Wang, J., 2007. Design and simulation study of a vacuum-pumping deaerating device for hydraulic oil. *Machine tool & hydraulics*, **35**(7):77-79 (in Chinese).

Khatib, O., Bowling, A., 1996. Optimization of the Inertial and Acceleration Characteristics of Manipulators. Proceedings of IEEE International Conference on Robotics and Automation, Minnesota, **4**(2883-2889). [doi:10.1109/ROBOT.1996.509150]

Kumar, V., 1992. Characterization of workspaces of parallel manipulators. *Journal of Mechanical Design*, **114**(3):368-375. [doi:10.1115/1.2926562]

Lebret, G., Liu, K., Lewis, F.L., 1993. Dynamic analysis and control of a Stewart platform Manipulator. *Journal of Robotic Systems*, **10**(5):629-655. [doi:10.1002/rob.4620100506]

Lou, Y.J., Liu, G.F., Li, Z.X., 2003. Optimal Design of Parallel Manipulators via LMI Approach. Proceedings of IEEE International Conference on Robotics and Automation, Taipei, **2**(1869-1874). [doi:10.1109/ROBOT.2003.1241867]

Merlet, J.P., 2002. Still a Long Way to Go on the Road for Parallel Mechanisms. ASME DETC Conference, Montréal, Canada.

Miller, K., 2004. Optimal design and modeling of spatial parallel manipulators. *The International Journal of Robotics Research*, **23**(2):127-140. [doi:10.1177/0278364904041322]

Pang, H., Shahinpoor, M., 1994. Inverse dynamics of a parallel manipulator. *Journal of Robotic Systems*, **11**(8):693-702. [doi:10.1002/rob.4620110803]

Pittens, K.H., Podhorodeski, R.P., 1993. A family of Stewart platforms with optimal dexterity. *Journal of Robotic Systems*, **10**(4):463-479. [doi:10.1002/rob.4620100405]

Ryu, J., Cha, J., 2001. Optimal Architecture Design of Parallel Manipulators for Best Accuracy. Proceedings of IEEE International Conference on Robotics and Systems, Hawaii, **3**(1281-1286). [doi:10.1109/IROS.2001.977159]

Shiller, Z., Sundar, S., 1991. Design of Robotic Manipulators for Optimal Dynamic Performance. Proceedings of IEEE International Conference on Robotics and Automation, Sacramento, **1**(334-339). [doi:10.1109/ROBOT.1991.132065]

Smaili, A.A., Diab, N.A., Atallah, N.A., 2005. Optimum synthesis of mechanisms using tabu-gradient search algorithm. *Journal of Mechanical Design*, **127**(5):917-923. [doi:10.1115/1.1904640]

Wang, H.R., 2001. Research for Motion and Force Control of Hydraulic 6-DOF Parallel Manipulator. Hebei University Press, Baoding, China (in Chinese).

Zhang, D., Gosselin, C.M., 2002. Parallel kinematic machine design with kinetostatic model. *Robotica*, **20**(4):429-438. [doi:10.1017/S0263574702004083]